Significance of the Fragmentation Region in Ultrarelativistic Heavy-Ion Collisions

B. B. Back,[1] M. D. Baker,[2] D. S. Barton,[2] R. R. Betts,[6] M. Ballintijn,[4] A. A. Bickley,[7] R. Bindel,[7] A. Budzanowski,[3] W. Busza,[4] A. Carroll,[2] M. P. Decowski,[4] E. García,[6] N. George,[1,2] K. Gulbrandsen,[4] S. Gushue,[2] C. Halliwell,[6] J. Hamblen,[8] G. A. Heintzelman,[2] C. Henderson,[4] D. J. Hofman,[6] R. S. Hollis,[6] R. Hołyński,[3] B. Holzman,[2] A. Iordanova,[6] E. Johnson,[8] J. L. Kane,[4] J. Katzy,[4,6] N. Khan,[8] W. Kucewicz,[6] P. Kulinich,[4] C. M. Kuo,[5] W. T. Lin,[5] S. Manly,[8] D. McLeod,[6] J. Michałowski,[3] A. C. Mignerey,[7] R. Nouicer,[6] A. Olszewski,[2,3] R. Pak,[2] I. C. Park,[8] H. Pernegger,[4] C. Reed,[4] L. P. Remsberg,[2] M. Reuter,[6] C. Roland,[4] G. Roland,[4] L. Rosenberg,[4] J. Sagerer,[6] P. Sarin,[4] P. Sawicki,[3] W. Skulski,[8] S. G. Steadman,[4] P. Steinberg,[2] G. S. F. Stephans,[4] M. Stodulski,[3] A. Sukhanov,[2] J.-L. Tang,[5] R. Teng,[8] A. Trzupek,[3] C. Vale,[4] G. J. van Nieuwenhuizen,[4] R. Verdier,[4] B. Wadsworth,[4] F. L. H. Wolfs,[8] B. Wosiek,[3] K. Woźniak,[3] A. H. Wuosmaa,[1] and B. Wysłouch[4]

[1]*Physics Division, Argonne National Laboratory, Argonne, Illinois 60439-4843, USA*
[2]*Chemistry and C-A Departments, Brookhaven National Laboratory, Upton, New York 11973-5000, USA*
[3]*Institute of Nuclear Physics, Kraków, Poland*
[4]*Laboratory for Nuclear Science, Massachusetts Institute of Technology, Cambridge, Massachusetts 02139-4307, USA*
[5]*Department of Physics, National Central University, Chung-Li, Taiwan*
[6]*Department of Physics, University of Illinois at Chicago, Chicago, Illinois 60607-7059, USA*
[7]*Department of Chemistry, University of Maryland, College Park, Maryland 20742, USA*
[8]*Department of Physics and Astronomy, University of Rochester, Rochester, New York 14627, USA*

(Received 5 October 2002; published 1 August 2003)

We present measurements of the pseudorapidity distribution of primary charged particles produced in Au + Au collisions at three energies, $\sqrt{s_{NN}} = 19.6$, 130, and 200 GeV, for a range of collision centralities. The distribution narrows for more central collisions and excess particles are produced at high pseudorapidity in peripheral collisions. For a given centrality, however, the distributions are found to scale with energy according to the "limiting fragmentation" hypothesis. The universal fragmentation region described by this scaling grows in pseudorapidity with increasing collision energy, extending well away from the beam rapidity and covering more than half of the pseudorapidity range over which particles are produced. This approach to a universal limiting curve appears to be a dominant feature of the pseudorapidity distribution and therefore of the total particle production in these collisions.

DOI: 10.1103/PhysRevLett.91.052303 PACS numbers: 25.75.Dw

The strong interaction, described by quantum chromodynamics (QCD), may be studied under conditions of high parton density and high energy density, using ultrarelativistic heavy ion collisions. The high density regime of QCD is sensitive to nonlinear dynamics and nonperturbative effects, including parton saturation, the onset of color deconfinement, and chiral symmetry restoration. More specifically, the pseudorapidity density of charged particles $dN_{\mathrm{ch}}/d\eta$, where $\eta \equiv -\ln\tan(\theta/2)$, is related to the entropy density at freeze-out. It has been demonstrated that the growth with energy of $dN_{\mathrm{ch}}/d\eta$ at midrapidity is modest compared to the original expectations [1,2] and provides a strong constraint on the initial state parton density and further particle production during the subsequent evolution of the system. This Letter focuses on particle production away from midrapidity, which constrains the collision dynamics more completely.

We have measured the pseudorapidity distribution of charged particles, $dN_{\mathrm{ch}}/d\eta$, over a broad range of η for Au + Au collisions at a variety of collision centralities (impact parameters). These measurements were made for three energies, $\sqrt{s_{NN}} = 19.6$, 130, and 200 GeV, covering a span of an order of magnitude in the same detector, allowing for a reliable systematic study of particle production with energy in these collisions. The data were taken using the PHOBOS apparatus [3] during the year 2000 and year 2001 runs of the Relativistic Heavy Ion Collider (RHIC) at Brookhaven National Laboratory. The apparatus used in this analysis comprises a set of silicon detectors covering $|\eta| < 5.4$, which are used for detecting the charged particles, and plastic scintillator counters, covering $3 < |\eta| < 4.5$, used for triggering.

The pseudorapidity densities $dN_{\mathrm{ch}}/d\eta$ were corrected for particles which were absorbed or produced in dead material and for feed-down products from weak decays of neutral strange particles. More details of the analysis procedures leading to the charged particle pseudorapidity density can be found in Ref. [4]. Two improvements in the handling of common-mode noise in the silicon detectors have been implemented for this analysis, leading to small changes in the results and to improved systematic errors. First, the event-by-event common-mode noise in the ring detectors ($3.0 < |\eta| < 5.4$) was found to grow with pad size, and the correction scheme was modified to include this effect. This refinement was already in place in Ref. [2]. Second, for very high occupancies, the common-mode noise correction in the octagon detector ($|\eta| < 3.2$) becomes slightly inaccurate. The more highly segmented

vertex detector was used to determine a correction factor for this effect in the octagon as a function of η, centrality, and beam energy. This correction was required only near midrapidity ($|\eta| < 1.5$) for the central data and it was less than 4% everywhere.

The centrality of the collision is characterized by the average number of nucleon participants $\langle N_{\rm part}\rangle$. For the 130 and 200 GeV data sets, this was estimated from the data using the truncated mean of the signals in two sets of 16 paddle counters covering $3 < |\eta| < 4.5$ forward and backward of the interaction point. In order to extract $\langle N_{\rm part}\rangle$ for a given fraction of the cross section, we rely on the fact that the multiplicity in the paddles increases monotonically with centrality. This assumption was verified using the neutral spectator energy measured in the forward hadronic calorimeters. In particular, we do not assume that the number of participants is proportional to the multiplicity.

At the lowest RHIC energy, $\sqrt{s_{NN}} = 19.6$ GeV, the much lower beam rapidity ($y_{\rm beam} \sim 3$) precludes the use of the paddle counters ($3 < |\eta| < 4.5$) for centrality determination. Instead, we construct a different quantity, "EOCT," which is approximately proportional to the multiplicity: the path-length corrected sum of the energy deposited in the octagon (silicon) detector ($|\eta| < 3.2$). Both HIJING simulations [5] and simple Glauber model [6,7] Monte Carlo simulations are used to estimate the fraction, ϵ, of the total cross section in the triggered sample, as well as to estimate the systematic error. Once ϵ is determined, cuts are made in EOCT in a similar way as with the paddle signal to extract $\langle N_{\rm part}\rangle$ for a chosen fraction of the total cross section [8]. As with the paddle signal, we assume only that EOCT is monotonic with $\langle N_{\rm part}\rangle$, not that it is proportional to it. The $\langle N_{\rm part}\rangle$ values and the estimated systematic uncertainties for various centrality bins and beam energies.

Figure 1 shows the charged particle pseudorapidity distributions ($dN_{\rm ch}/d\eta$) measured at $\sqrt{s_{NN}} = 200$, 130, and 19.6 GeV for different centrality bins for $-5.4 < \eta < 5.4$. Because of the large acceptance of the detector, $dN_{\rm ch}/d\eta$ is measured over almost the full range of η, except for a small missing fraction at very high $|\eta|$. Using data at lower energy (see Fig. 2), this fraction is estimated to be less than 2% for the 130 and 200 GeV central (0%–6%) results. Table II lists the integrated charged multiplicity for three energies in different ranges of η. The fiducial range $|\eta| < 4.7$ is quoted for easier comparison to data from the BRAHMS experiment [9,10]. The remaining columns show the integral over the full PHOBOS fiducial range $|\eta| < 5.4$, and the total inferred $N_{\rm ch}$.

After scaling by $\langle N_{\rm part}\rangle$ to correct for the slight differences in centrality binning, the 130 and 200 GeV BRAHMS data are shown to be about 6% lower than the PHOBOS data, consistent within errors. The comparison of the 19.6 GeV Au + Au RHIC collider data with CERN Pb + Pb fixed target data ($\sqrt{s_{NN}} = 17.2$ GeV) takes some care. For instance, using NA49 data [11], we find that the midrapidity value of $dN/d\eta$ depends on the frame: $dN/d\eta_{\rm cm}$ is 15%–20% lower than $dN/d\eta_{\rm lab}$. To make the comparison with PHOBOS, the $d^2N/dydp_T$ data for each particle species can be reassembled in the cm frame. For NA49, this leads to $dN_{\rm ch}/d\eta_{\rm cm}/\langle N_{\rm part}/2\rangle|_{|\eta|<0.6} \approx 10.9$. Scaled by the energy dependence [2], this leads to an expectation of 2.0 for 19.6 GeV, remarkably consistent with the PHOBOS result of 2.06 ± 0.23. The WA98 [12] and NA50 [13] results are 10% and 5% higher than NA49, respectively, also consistent with PHOBOS. The older EMU-13 result [14] is about 20% lower than NA49 and is therefore inconsistent with PHOBOS.

Taking advantage of the large pseudorapidity coverage of PHOBOS, we can study the properties of the fragmentation region by viewing the data at different energies in the rest frame of one of the colliding nuclei. Such an approach led to the ansatz of limiting fragmentation [15], which successfully predicted the energy dependence of particle production away from midrapidity in hadron collisions, including $p + \bar{p}$ [16], and both $p + A$ and $\pi + A$ collisions [17]. This ansatz states that, at high enough collision energy, both $d^2N/dy'dp_T$ and the mix of particle species reach a limiting value and become independent of energy in a region around $y' \sim 0$, where $y' \equiv y - y_{\rm beam}$ and rapidity $y \equiv \tanh^{-1}\beta_z$. The limiting value for $d^2N/dy'dp_T$ and particle mix also implies a limiting value for $dN/d\eta'$ where $\eta' \equiv \eta - y_{\rm beam}$.

Figure 2(a) shows the scaled, shifted pseudorapidity distributions $dN_{\rm ch}/d\eta'/\langle N_{\rm part}/2\rangle$ for central Au + Au

TABLE I. Estimated number of nucleon participants (and systematic error) for 19.6 and 130 GeV Au + Au collisions according to the centrality bin (quoted as a fraction of the inelastic cross section).

Cent.	$\langle N_{\rm part}^{19.6}\rangle$	$\langle N_{\rm part}^{130}\rangle$	$\langle N_{\rm part}^{200}\rangle$	Cent.	$\langle N_{\rm part}^{19.6}\rangle$	$\langle N_{\rm part}^{130}\rangle$	$\langle N_{\rm part}^{200}\rangle$
0%–6%	337 ± 12	340 ± 11	344 ± 11	10%–15%	247 ± 11	258 ± 8	256 ± 8
6%–15%	265 ± 11	275 ± 9	274 ± 9	15%–20%	210 ± 12	215 ± 8	217 ± 8
15%–25%	194 ± 12	196 ± 8	200 ± 8	20%–25%	178 ± 12	178 ± 7	183 ± 7
25%–35%	138 ± 13	136 ± 6	138 ± 6	25%–30%	150 ± 13	148 ± 6	152 ± 6
35%–45%	···	90 ± 5	93 ± 5	30%–35%	125 ± 13	124 ± 6	124 ± 6
0%–3%	351 ± 14	354 ± 12	358 ± 12	35%–40%	103 ± 14	100 ± 5	103 ± 5
3%–6%	322 ± 10	327 ± 10	331 ± 10	40%–45%	···	80 ± 5	83 ± 5
6%–10%	287 ± 10	298 ± 9	298 ± 9	45%–50%	···	64 ± 4	65 ± 4

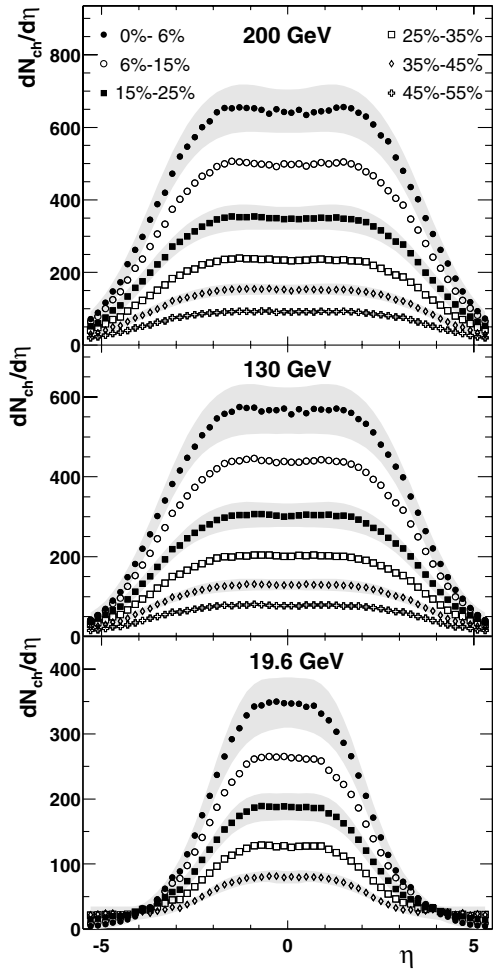

FIG. 1. The charged particle pseudorapidity distribution, $dN_{\rm ch}/d\eta$, measured for Au + Au at $\sqrt{s_{NN}} = 200$, 130, and 19.6 GeV for the specified centrality bins. Note: the 45%–55% bin is not reported for the 19.6 GeV data due to uncertainties caused by the very low multiplicity in these events. The typical systematic errors (90% C.L.) are shown as bands for selected centrality bins. The statistical errors are negligible.

collisions which span a factor of 10 in collision energy ($\sqrt{s_{NN}}$). The results are folded about midrapidity (positive and negative η bins are averaged). The distributions are observed to be independent of collision energy over a substantial η' range. This is consistent with and extends a similar observation made by BRAHMS [10] over a more restricted η' range. Both the 19.6 and 130 GeV data reach 85%–90% of their maximum value before deviating significantly (more than 5%) from the common limiting curve. These data demonstrate that limiting fragmentation applies well in the Au + Au system and that the "fragmentation region" is rather broad, covering more than half of the available range of η' over which particles are produced. In particular, the fragmentation region grows significantly between 19.6 and 130 GeV, extending more than two units away from the beam rapidity. A similar effect was observed in $p + \bar{p}$ collisions, over a range of $\sqrt{s}$ from 53 to 900 GeV [16]. In both cases,

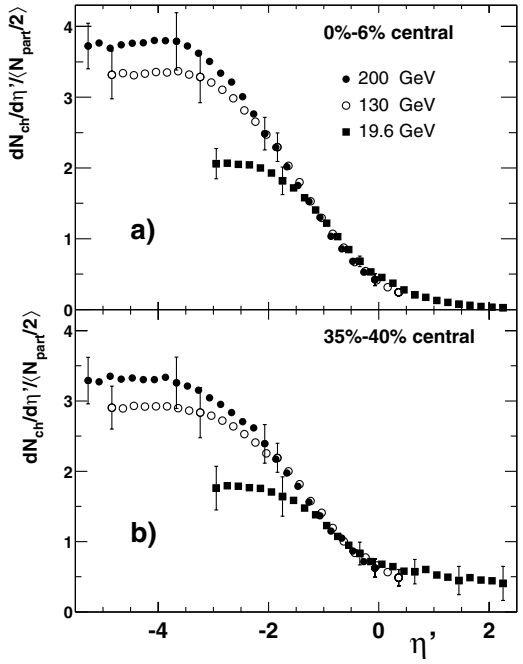

FIG. 2. Au + Au data for $\sqrt{s_{NN}} = 19.6$, 130, and 200 GeV, plotted as $dN_{\rm ch}/d\eta'$ per participant pair, where $\eta' \equiv \eta - y_{\rm beam}$ for (a) 0%–6% central and (b) 35%–40% central. Systematic errors (90% C.L.) are shown for selected, typical, points.

particle production appears to approach a fixed limiting curve which extends far from the original beam rapidity, indicating that this universal curve is an important feature of the overall interaction and not simply a nuclear breakup effect. This result is in sharp contrast to the boost-invariance scenario [18] which predicts a fixed fragmentation region and a broad central rapidity plateau that grows in extent with increasing energy.

Figure 2(b) shows the scaled pseudorapidity distributions for a set of noncentral collisions, which also exhibit limiting fragmentation over a broad range of η'. Figure 3 shows the centrality dependence of the $dN_{\rm ch}/d\eta'/\langle N_{\rm part}/2\rangle$ distribution at the two extreme energies: 19.6 and 200 GeV. These data demonstrate that particle production in the fragmentation region changes significantly with centrality. Figure 4 shows the ratio of noncentral to central data with (90% C.L.) systematic errors included. The error in the ratio involves a partial cancellation of the systematic errors in the individual measurements. For $\eta' > -1.5$, the scaled pseudorapidity density actually grows in the peripheral data with respect to the more central data. This effect has already been observed for

TABLE II. Total charged multiplicity in three fiducial ranges of η for central (0%–6%) collisions.

$\sqrt{s_{NN}}$	$N_{\rm ch}(\lvert\eta\rvert < 4.7)$	$N_{\rm ch}(\lvert\eta\rvert < 5.4)$	$N_{\rm ch}$(total)
19.6 GeV	1670 ± 100	1680 ± 100	1680 ± 100
130 GeV	4020 ± 200	4100 ± 210	4170 ± 210
200 GeV	4810 ± 240	4960 ± 250	5060 ± 250

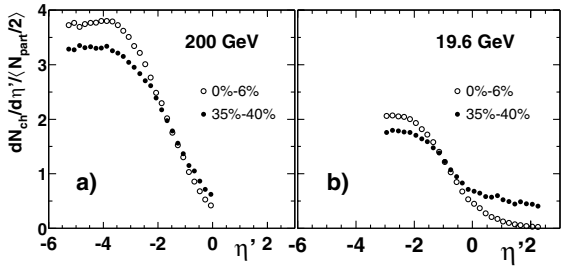

FIG. 3. The distribution $dN_{\rm ch}/d\eta'$ per participant pair for central (0%–6%) and noncentral (35%–40%) Au + Au collisions for (a) $\sqrt{s_{NN}} = 200$ GeV and (b) $\sqrt{s_{NN}} = 19.6$ GeV. Systematic errors are not shown.

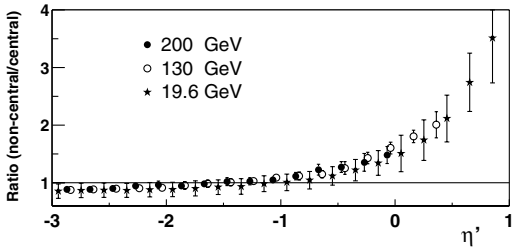

FIG. 4. The ratio of $dN_{\rm ch}/d\eta'$ per participant pair between noncentral (35%–40%) and central (0%–6%) data plotted for $\sqrt{s_{NN}} = 200$, 130, and 19.6 GeV. The errors represent a 90% C.L. systematic error on the ratio.

Au + Au collisions at $\sqrt{s_{NN}} = 130$ GeV [4] and for Pb+Pb collisions at 17.2 GeV [14]. This contradicts the suggestion, put forward in Refs. [9,10], that the limiting curve for particle production in the fragmentation region is independent of centrality as well as of energy. It should be noted that the hypothesis of limiting fragmentation does not imply that the limiting curve is independent of centrality, just that $dN_{\rm ch}/d\eta'/\langle N_{\rm part}/2\rangle$ is energy independent for a fixed centrality, once at sufficiently high energy.

The strong centrality dependence seen in Fig. 3 has two features: an excess of particles at high η in peripheral Au + Au events and a narrowing of the overall pseudorapidity distribution. The excess of particles at high $|\eta|$ can be most easily seen in Fig. 1, where, for the 19.6 GeV data, the absolute yield of charged particles actually grows for noncentral collisions. It should be noted that the very peripheral limit of a Au + Au collision is *not* an N + N collision, but rather an N + N collision with two large excited nuclear remnants. The increased particle production due to the nuclear remnants has been studied in lower energy Pb + Pb collisions [14] and in $p + A$ collisions [17]. The narrowing of the overall distribution may be due to dynamical effects, such as baryon stopping [19], or kinematic effects, such as a shift in η' (for fixed y') due to the particle mix (p/π ratio) changing with centrality. This narrowing of the distribution can be characterized as an increase at midrapidity [8,20] with an approximately compensating reduction at high η.

In summary, we have performed a comprehensive examination of the pseudorapidity distributions of charged particles produced in Au + Au collisions at RHIC energies from $\sqrt{s_{NN}} = 19.6$ to 200 GeV, including an estimate of the full charged particle multiplicity at three energies. For central collisions at the highest energy, we find that a total of more than 5000 charged particles are produced. These results span 11 units of pseudorapidity, a factor of 10 in energy, and a factor of 5 in $\langle N_{\rm part}\rangle$ — all measured in a single detector. The data show a number of interesting features. First, limiting fragmentation (energy independence of $dN/d\eta'$) is valid over a large range of η'. Second, the scaled $dN/d\eta$ shape is not independent of centrality at high η. The η distribution is broader in peripheral collisions than in central collisions. Third, as in $p + \bar{p}$ collisions, the fragmentation region in Au + Au collisions grows in pseudorapidity extent with beam energy, becoming a dominant feature of the pseudorapidity distributions at high energy.

We thank the BNL directorate and the C-A department for providing the variety of collision energies at RHIC which made this work possible. This work was partially supported by U.S. DoE Grants No. DE-AC02-98CH10886, No. DE-FG02-93ER40802, No. DE-FC02-94ER40818, No. DE-FG02-94ER40865, No. DE-FG02-99ER41099, No. W-31-109-ENG-38, by U.S. NSF Grants No. 9603486, No. 9722606, No. 0072204, by Polish KBN Grant No. 2-P03B-10323, and by NSC of Taiwan Contract No. NSC 89-2112-M-008-024.

[1] B. B. Back *et al.*, Phys. Rev. Lett. **85**, 3100 (2000).
[2] B. B. Back *et al.*, Phys. Rev. Lett. **88**, 22302 (2002).
[3] B. B. Back *et al.*, Nucl. Instrum. Methods Phys. Res., Sect. A **499**, 603 (2003).
[4] B. B. Back *et al.*, Phys. Rev. Lett. **87**, 102303 (2001).
[5] X. N. Wang and M. Gyulassy, Phys. Rev. D **44**, 3501 (1991).
[6] W. Czyz and L. C. Maximon, Ann. Phys. (N.Y.) **52**, 59 (1969).
[7] R. J. Glauber and G. Matthiae, Nucl. Phys. **B21**, 135 (1970).
[8] B. B. Back *et al.*, Phys. Rev. C **65**, 061901R (2002).
[9] I. G. Bearden *et al.*, Phys. Lett. B **523**, 227 (2001).
[10] I. G. Bearden *et al.*, Phys. Rev. Lett. **88**, 202301 (2002).
[11] H. Appelhaüser *et al.*, Phys. Rev. Lett. **82**, 2471 (1999); S. F. Afanasiev *et al.*, Phys. Rev. C **66**, 054902 (2002).
[12] M. M. Aggarwal *et al.*, Eur. Phys. J. C **18**, 651 (2001).
[13] M. C. Abreu *et al.*, Phys. Lett. B **530**, 33 (2002); **530**, 43 (2002).
[14] P. Deines-Jones *et al.*, Phys. Rev. C **62**, 014903 (2000).
[15] J. Benecke, T. T. Chou, C-N. Yang, and E. Yen, Phys. Rev. **188**, 2159 (1969).
[16] G. J. Alner *et al.*, Z. Phys. C **33**, 1 (1986).
[17] J. E. Elias *et al.*, Phys. Rev. D **22**, 13 (1980).
[18] J. D. Bjorken, Phys. Rev. D **27**, 140 (1983).
[19] W. Busza and A. S. Goldhaber, Phys. Lett. **139B**, 235 (1984).
[20] B. B. Back *et al.*, Phys. Rev. C **65**, 031901R (2002).